# PROCESSING OF COMPOSITES

Edited by
Raju S. Davé and Alfred C. Loos

Series Editor: Warren Baker

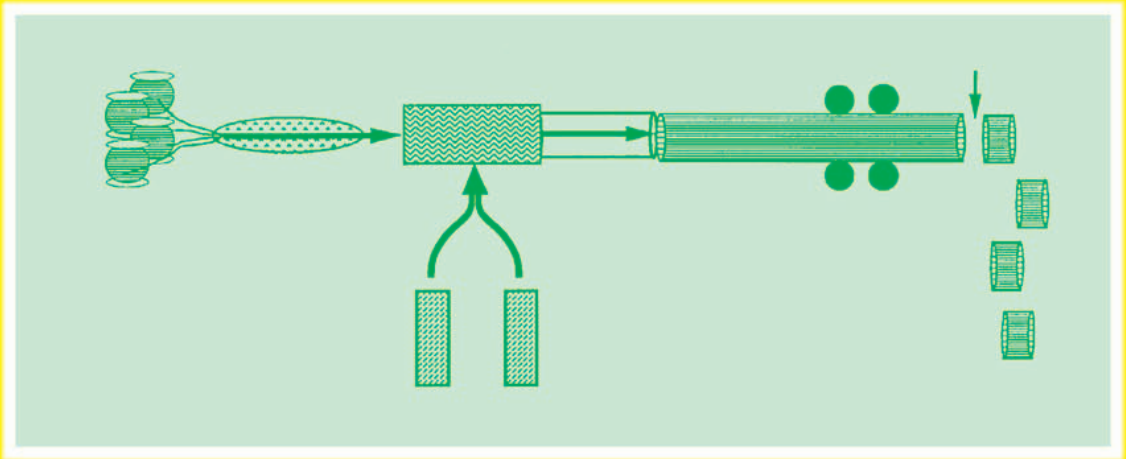

HANSER

*Raju S. Davé / Alfred C. Loos*

# Processing of Composites

**Polymer Processing Society**

## Progress in Polymer Processing

*Series Editor: L.A. Utracki*

A.I. Isayev
**Modelling of Polymer Processing**

L.A. Utracki
**Two-Phase Polymer Systems**

A. Singh/J. Silvermann
**Radiation Processing of Polymers**

*Series Editor: W.E. Baker*

I. Manas-Zloczower/Z. Tadmor
**Mixing and Compounding of Polymers**

T. Kanai/G.A. Campbell
**Film Processing**

R.S. Davé/A.C. Loos
**Processing of Composites**

*R.S. Davé/A.C. Loos (Editors)*

# Processing of Composites

With Contributions from

F. Abrams, S.G. Advani, B.T. Åström, V.M.A. Calado,
F.C. Campbell, D. Cohen, R.S. Davé,
B.R. Gebart, B. Joseph, J.L. Kardos, B. Khomami,
S.C. Kim, D.E. Kranbuehl, R.L. Kruse, M-C Li,
A.C. Loos, A.R. Mallow, S.C. Mantell, A.K. Miller,
J.W. Park, L.A. Strömbeck, M.M. Thomas,
K. Udipi, and S.R. White


Hanser Publishers, Munich

Hanser/Gardner Publications, Inc., Cincinnati

The Editors:
*Raju S. Davé*, Morrison & Foerster, 2000 Pennsylvania Avenue NW, Washington, DC 20006-1888, USA
*Alfred C. Loos*, Department of Engineering Science and Mechanics, Virginia Polytechnic Institute and State University, Blacksburg, VA 24061, USA

Distributed in the USA and in Canada by
Hanser/Gardner Publications, Inc.
6915 Valley Avenue, Cincinnati, Ohio 45244-3029, USA
Fax: (513) 527-8950
Phone: (513) 527-8977 or 1-800-950-8977
Internet: http://www.hansergardner.com

Distributed in all other countries by
Carl Hanser Verlag
Postfach 86 04 20, 81631 München, Germany
Fax: +49 (89) 98 12 64



Library of Congress Cataloging-in-Publication Data
Processing of composites / Raju S. Davé, Alfred C. Loos, editors :
with contributions from F. Abrams . . . [et al.].
p. cm. – (Progress in polymer processing)
Includes bibliographical references and index.
ISBN 1-56990-226-7 (hc.)
1. Plastics. 2. Polymeric composites. I. Davé, Raju S.
II. Loos, Alfred C. III. Series.
TP1120.P76 1999
668.4—dc21 99-27337

Die Deutsche Bibliothek – CIP-Einheitsaufnahme
Processing of composites / Raju S. Davé/Alfred C. Loos (ed.). With contributions from F. Abrams . . . – Munich : Hanser ; Cincinnati : Hanser/Gardner, 1999
(Progress in polymer processing)
ISBN 3–446-18044-3


Typeset in England by Techset Composition Ltd., Salisbury
Printed and bound in Germany by Kösel, Kempten

**PROGRESS IN POLYMER PROCESSING SERIES**

Warren E. Baker, *Series Editor*

## Advisory Board

# Foreword

Since World War II, the industry based on polymeric materials has developed rapidly and spread widely. The polymerization of new polymeric species advanced rapidly during the 1960s and 1970s, providing a wide range of properties. A plethora of specialty polymers have followed as well, many with particularly unique characteristics. This evolution has been invigorated by the implementation of metallocene catalyst technology. The end use of these materials has depended on the development of new techniques and methods for forming, depositing, and locating these materials in advantageous ways, which are usually quite different from those used by the metal or glass fabricating industries. The importance of this activity, "polymer processing," is frequently underestimated when reflecting on the growth and success of the industry.

Polymer processes, such as extrusion, injection molding, thermoforming, and casting provide parts and products with specific shapes and sizes. Furthermore, they must control, beneficially, many of the unusual and complex properties of these unique materials. Because polymers have high molecular weights and, in may cases, tend to crystallize, polymer processes are called to control the nature and extent of orientation and crystallization, which, in turn, have a substantial influence on the final performance of the products made. In some cases, these processes involve synthesizing polymers during the polymer processing operation, such as continuous fiber composites processing, which is the topic of this book. Autoclave processing, pultrusion, and filament winding each synthesize the polymer and form a finished part in one step or a sequence of steps, evidence of the increasing complexity of the industry. For these reasons, successful polymer process researchers and engineers must have a broad knowledge of fundamental principles and engineering solutions.

Some polymer processes have flourished in large indutrial units, such as synthetic fiber spinning. However the bulk of the processes are rooted in small- and medium-sized entrepreneurial enterprises in both developed and new developing countries. Their energy and ingenuity have sustained growth to this point, but clearly the future will belong to those who progressively adapt new scientific knowledge and engineering principles to the industry. Mathematical modeling, online process control and product monitoring, and characterization based on the latest scientific techniques will be important tools in keeping these organizations competitive in the future

The Polymer Processing Society was started in Akron, Ohio, in 1985 with the aim of focusing on an international scale on the development, discussion, and dissemination of new and improved polymer processing technology. The society facilitates this by sponsoring several conferences annually and by publishing the journal, *International Polymer Processing*, and this book series, *Progress in Polymer Processing*. This series of texts is dedicated to the goal of bringing together the expertise of accomplished academic and industrial professionals. The volumes have a multiauthored format, which provides a broad picture of the volume topic viewed from the perspective of contributors from around the world. To accomplish these goals, we need the thoughtful insight and effort of our authors and

book editors, the critical overview of our Editorial Board, and the efficient production of our publisher.

The book deals with the underlying process fundamentals and manufacturing processes for preparing polymer composites reinforced with continuous fibers. These processes have developed into what is arguably the single largest producer of complex engineered parts, finding significant application in the aerospace industry, for example. The resulting products represent the most significant incursion by polymeric materials into those areas, where high performance traditional materials, such as metals and ceramics, have been used. These achievements are dependent on the complex interplay of chemical kinetics, rheology, and morphology development in a multiphase environment, which leads to the required anisotropic properties. Quite new continuous fiber composite processes have been developed during the last decade, and the complexity and fundamental steps involved signal further imaginative developments in the future. This book includes numerous contributions, industrial and institutional, from America as well as Europe and Asia and, as such, forms a valuable contribution to the field.

Brampton, Ontario, Canada

*Warren E. Baker*
*Series Editor*

# Contents

# Contributors

*Abrams, F.*, WL/MLBC, Wright Patterson Air Force Base, 011 45433-7750, USA

*Advani, Suresh G.*, Department of Mechanical Engineering, University of Delaware, Newark, DE 19716-3140, USA

*Åström, B.T.*, Department of Lightweight Structures, Royal Institute of Technology, Stockholm, Sweden

*Calado, Verônica M.A.*, Department of Chemical Engineering, University of Rio de Janeiro, Rio de Janeiro 21949-900, Brazil

*Campbell, Flake C.*, Materials Directorate, Wright Laboratories, Charles B. Browning Air Force Base, Dayton, OH 45433, USA

*Cohen, D.*, Hercules Aerospace Company, Magna, UT 84044-0094, USA

*Davé, Raju S.,* c/o Morrison & Foerster, 2000 Pennsylvania Avenue NW, Washington, DC 20006-1888, USA

*Gebart, B. Rikard*, Swedish Institute of Composites, 8-941 26 Pitea, Sweden

*Joseph, Babu*, Materials Research Laboratory, School of Engineering and Applied Science, Washington University, St. Louis, MO 63130-4899, USA

*Kardos, J.L.*, Department of Chemical Engineering, Washington University, St. Louis, MO 63130-4899, USA

*Khomami, Bamin*, Department of Chemical Engineering, Washington University, St. Louis, MO 63130-4899, USA

*Kim, S.C.*, Department of Chemical Engineering, Korea Advanced Institute of Science and Technology, Taejon 305-701, Korea

*Kranbuehl, David E.*, Departments of Chemistry and Applied Science, College of William and Mary, Williamsburg, VA 23187-8795, USA

*Kruse, Robert L.*, 444 Michael Sears Toad, Belchertown, MA 01007, USA

*Li, Min-Chung*, Impco Technologies, Cerritos, CA 90701, USA

*Loos, Alfred C.*, Department of Engineering Science and Mechanics, Virginia Polytechnic Institute and State University, Blacksburg, VA 24061, USA

*Mallow, Andrew R.*, McDonnell Douglas Aerospace, St. Louis, MO 63146-4021, USA

*Mantell, S.C.*, Department of Mechanical Engineering, University of Minnesota, Minneapolis, MN 55455, USA

*Miller, Alan K.*, Lockheed-Martin Missiles and Space, Sunnyvale, CA 94088, USA

*Park, J.W.*, Department of Chemical Engineering, Korea Advanced Institute of Science and Technology, Taejon 305-701, Korea

*Strömbeck, L. Anders*, Borealis Industries, 42246 Hisingsbacka, Sweden

*Thomas, Matthew M.*, Department of Chemical Engineering, Washington University, St. Louis, MO 63130-4899, USA

*Udipi, Kishore*, Monsanto Company, St. Louis, MO 63167, USA

*White, Scott R.*, University of Illinois, Urbana-Champaign, Urbana, IL 61801, USA

# Preface

Composite materials have been acclaimed as the "Materials of the Future." A key question is whether composite materials will always remain the materials of the future or if the future is here. Advanced polymer composites, once destined for stealth military aircraft or aerospace uses, are beginning to be used in down-to-earth structures, such as bridges, buildings, and highways. However, there are still considerable impediments to wider use, and composite manufacturers need to make great strides in the development and manufacturing of composite materials.

What makes the fabrication of composite materials so complex is that it involves simultaneous heat, mass, and momentum transfer, along with chemical reactions in a multiphase system with time-dependent material properties and boundary conditions. Composite manufacturing requires knowledge of chemistry, polymer and material science, rheology, kinetics, transport phenomena, mechanics, and control systems. Therefore, at first, composite manufacturing was somewhat of a mystery because very diverse knowledge was required of its practitioners. We now better understand the different fundamental aspects of composite processing so that this book could be written with contributions from many composite practitioners.

This book provides a quick overview of the fundamental principles underlying composite processing and summarizes a few important processes for composite manufacturing. This book is intended for those who want to understand the fundamentals of composite processing. In particular, this book would be especially valuable for students as a graduate level textbook and practitioners who struggle to optimize these processes.

We thank all the chapter authors for their heroic efforts in writting their chapters. Without their contributions this book would be incomplete. In addition, we thank Lloyd Goettler of Monsanto, who is past president of the Polymer Processing Society, for suggesting that we edit this book. Other friends and mentors who had a major influence on our work include Robert L. Kruse, Kishore Udipi, and Allen Padwa, all of Monsanto, and Professor John L. Kardos of Washington University. Professor Warren Baker, Series Editor, has been very helpful in overseeing this project.

Certainly, we may have overlooked others who have helped us on our way to completing this book over a period of four years. Our sincere apologies to them, and we hope they will reflect on their positive contributions when they read this book. Last, but not least, we thank our families who endured through this process. Criticism and comments from readers are most welcome.

*Raju S. Davé*
*Alfred C. Loos*

# Part I
# Theory

# 1 Chemistry, Kinetics, and Rheology of Thermoplastic Resins Made by Ring Opening Polymerization*

**Raj S. Davé†, Kishore Udipi, and Robert L. Kruse‡**



*The ring opening polymerization of cyclic monomers that yield thermoplastic polymers of interest in composite processing is reviewed. In addition, the chemistry, kinetics, and rheology of the ring opening polymerization of caprolactam to nylon 6 are presented. Finally, the rheo-kinetics models for polycaprolactam are applied to the composite process of reaction injection pultrusion.*

## 1.1 Overview

Ring opening polymerization of cyclic monomers to yield thermoplastic polymers has been studied by a number of investigators [1–19] over the years. A variety of cyclic monomers ranging in structures from the more commonly encountered olefins, ethers, formals, lactones,

* Work done in Monsanto Plastics Division and approved by Monsanto Company for external publication.
† Formerly with Monsanto Plastics and Bayer Polymers and to whom correspondence should be addressed.
‡ Formerly with Monsanto Plastics.

lactams, and carbonates to some of the more esoteric, like the thioformals, thiolactones, iminoethers, siloxanes, cyclic phosphites, cyclic phosphonites, and phosphonitrilic chloride have been polymerized to generate thermoplastics that range in properties from soft elastomeric to hard and crystalline.

All ring opening polymerizations are governed by ring-chain equilibria. Tendency toward polymerization of a cyclic monomer depends upon the existence and extent of ring strain, the initiator used, and the reactivity of the functional group within the ring [20]. Ring strain, which is a thermodynamic property, is generated in a cyclic monomer by the angular distortion of the chemical bonds and the steric effects of the substituents. The lower the ring strain, the more stable is the monomer with lower tendency to polymerize.

The thermodynamics of ring opening polymerization was first proposed by Dainton and Ivin [21] in the form of the following expression:

$$T_c = \frac{\Delta H_p}{\Delta S_p + R \ln[M]} \tag{1.1}$$

where $T_c$ is the ceiling temperature (above which polymerization at monomer concentration $[M]$ is not possible), $\Delta H_p$ and $\Delta S_p$ are the enthalpy and entropy changes of polymerization, respectively, and $R$ is the universal gas constant. It follows from Equation 1.1 that a lower temperature favors polymerization.

Most cyclic monomers of interest in the field of composites happen to be heterocyclic in nature. Polymerizability of some monomers is summarized in Table 1.1. Ring opening polymerizations invariably follow ionic mechanisms, although a few are known to proceed via the free radical route and some via metathesis involving metallocarbene intermediates.

Among the more common thermoplastics from ring opening polymerization of interest in composite processing are polylactams, polyethers, polyacetals, and polycycloolefins. It has also been shown that polycarbonates can be produced from cyclic carbonates [22]. Anionic ring opening polymerization of caprolactam to nylon 6 is uniquely suited to form a thermoplastic matrix for fiber-reinforced composites, specifically by the reaction injection pultrusion process [23–25]. The fast reaction kinetics with no by-products and the crystalline

**Table 1.1 Polymerizability of Some Unsubstituted Cyclic Monomers**

| | Polymerizability | | |
|---|---|---|---|
| | Ring size | | |
| Class of monomer | Five | Six | Seven |
| Lactam | + | + | + |
| Lactone | + | + | + |
| Imide | − | − | + |
| Anhydride | − | − | + |
| Ethers | + | − | + |

+ = polymerizes
− = does not polymerize

nature of the nylon so produced make anionic polymerization of caprolactam a compelling choice for the reaction injection pultrusion process. In addition to the fast reaction kinetics, low viscosity of the monomer affords superior wetting of the reinforcing fibers, which leads to improved adhesion between the fibers and the matrix polymer, as compared with the conventional thermoplastic composite processes where the melt viscosity of the thermoplastic polymers is too high to afford good wetting of the fibers. Because this chapter will later cover polylactams in greater detail, the chemistry of other thermoplastic polymers by ring opening polymerization will be dealt with here in some detail.

Polyethers are prepared by the ring opening polymerization of three, four, five, seven, and higher member cyclic ethers. Polyalkylene oxides from ethylene or propylene oxide and from epichlorohydrin are the most common commercial materials. They seem to be the most reactive alkylene oxides and can be polymerized by cationic, anionic, and coordinated nucleophilic mechanisms. For example, ethylene oxide is polymerized by an alkaline catalyst to generate a living polymer in Figure 1.1. Upon addition of a second alkylene oxide monomer, it is possible to produce a block copolymer (Fig. 1.2).

Cationic polymerization of alkylene oxides generally produces low molecular weight polymers, although some work [26] seems to indicate that this difficulty can be overcome by the presence of an alcohol (Fig. 1.3). Higher molecular weight polyethylene oxides can be prepared by a coordinated nucleophilic mechanism that employs such catalysts as alkoxides, oxides, carbonates, and carboxylates, or chelates of alkaline earth metals (Fig. 1.4). An aluminum-porphyrin complex is claimed to generate 'immortal' polymers from alkylene oxides that are totally free from termination reaction [27].

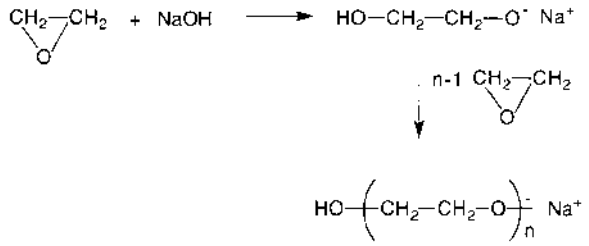


Figure 1.1 Living polymerization of ethylene oxide

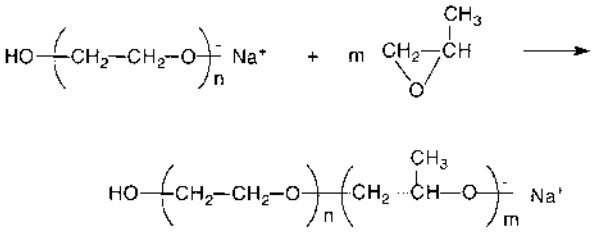


Figure 1.2 Block copolymer of ethylene oxide and propylene oxide

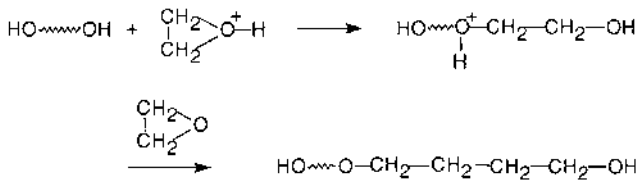

Figure 1.3 Cationic polymerization of ethylene oxide in the presence of an alcohol

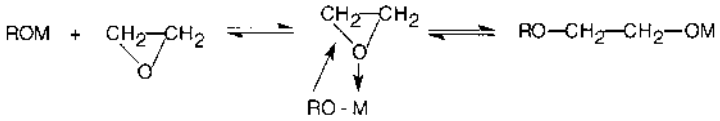

Figure 1.4 Polymerization of ethylene oxide by nucleophilic mechanism

Tetrahydrofuran, a five-member cyclic ether, polymerizes cationically to yield an elastomeric polymer [28]. Oxepane, a seven-member analog, polymerizes to a crystalline polymer.

By organic chemistry formalism, polyacetals are reaction products of aldehydes with polyhydric alcohols. Polymers generated from aldehydes, however, either via cationic or anionic polymerization are generally known as *polyacetals* because of repeating acetal linkages. Formaldehyde polymers, which are commercially known as *acetal resins*, are produced by the cationic ring opening polymerization of the cyclic trimer of formaldehyde, viz., trioxane [29–30] (Fig. 1.5).

Polyacetals are prone to degrade to the monomers at elevated temperatures by an unzipping mechanism. They are either end-capped or copolymerized with low levels of an alkylene oxide to prevent unzipping and impart better processability. Polyacetals from higher aldehydes do crystallize, with the degree of crystallinity depending upon the length of the side chain, *R* (Fig. 1.6). The longer the side chain, the less crystalline is the material and the lower is the melting. Polyformals are prepared by the cationic ring opening polymerization of cyclic formals. These could be regarded as codimers of formaldehyde and cyclic ethers. Thus, polyformals correspond to alternating copolymers of aldehydes and cyclic ethers.

Polycycloolefins are prepared by ring opening metathesis polymerization (ROMP) using transition metal catalysts [31]. By far the most commonly studied monomer is dicyclopentadiene (Fig. 1.7). Cycloolefins with high ring strains like norbornenes and their analogs polymerize very fast and the polymerizations are quite exothermic. Metathesis catalyst systems tend to be sensitive to the presence of polar compounds and the polymerization rates

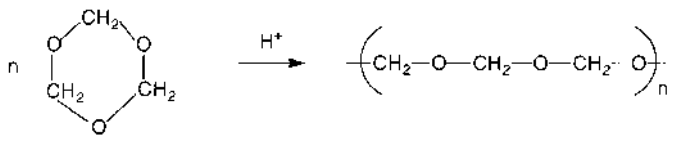

Figure 1.5 Cationic ring opening polymerization of a cyclic trimer of formaldehyde (viz., trioxane)

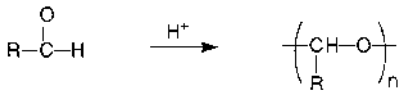

Figure 1.6 Polyacetals from higher aldehydes

are adversely affected. In the case of norbornenes, however, because of the highly strained ring, such catalyst systems appear to be more forgiving.

Polycarbonates, both aliphatic and aromatic, have been prepared by the ring opening polymerization of cyclic monomers or oligomers [22]. Cyclic monomeric precursors are more common in aliphatic polycarbonates, but because of steric reasons aromatic polycarbonates can only be prepared from cyclic oligomers. Both cationic and anionic initiators have been examined and anionic initiators appear to be more efficient.

Although aliphatic polycarbonates have been prepared and studied quite extensively, interest in them has been minimal due to their thermal instability and, in some cases, lack of ductility. Aliphatic polycarbonates with $\beta$ hydrogens decompose to olefins, alcohol, and $CO_2$.

Attempts to prepare aromatic polycarbonates from cyclic oligomers had continued through the years without much success. Researchers at General Electric have developed a method that would afford much more control over the composition of the oligomers than ever before [22]. In this process, a bisphenol A-bischloroformate is added slowly to an efficiently stirred mixture of $Et_3N$, aqueous NaOH, and $CH_2Cl_2$ to selectively control the hydrolysis/condensation to generate a mixture of essentially cyclic oligomers and high molecular weight polymer ($\sim$85/15) with extremely low levels of linear oligomers (Fig. 1.8). This procedure provides a distribution of oligomers of $n = 2$–26 with $>$90% species with degrees of polymerization $<$10.

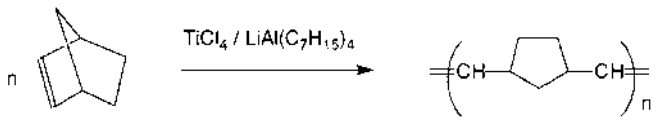

Figure 1.7 Ring opening metathesis polymerization of dicyclopentadiene using transition metal catalysts

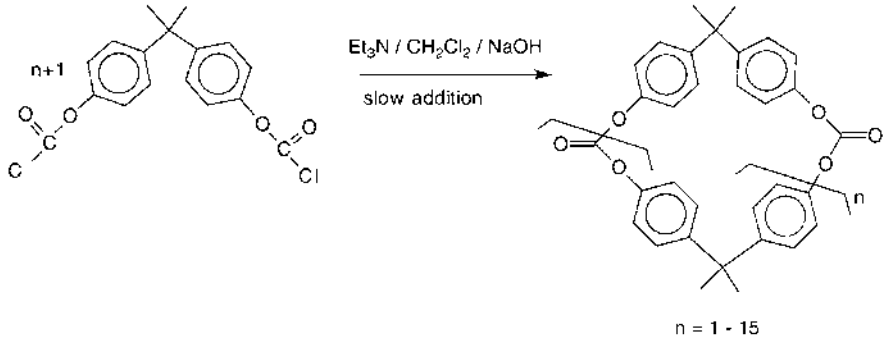

Figure 1.8 Preparation of cyclic oligomers that yield polycarbonates by ring opening polymerization

Heating these cyclic oligomers to 300°C for about 30 minutes results in ring opening polymerization to polycarbonates. The molecular weights of the resulting polycarbonates prepared in the absence of a catalyst are modest (< 20,000), whereas catalysts like lithium stearate or titanium alkoxides produce polycarbonates of much higher molecular weights (50,000–300,000).

## 1.2 Chemistry of Anionic Ring Opening Polymerization of Lactams

Anionic ring opening polymerization of lactams to generate polyamides has been studied quite extensively by Sebenda [8–10], Sekiguchi [11], and Wichterle [12–13], among others, in academia, and by Gabbert and Hedrick [14] and by us [23–25] in industry. By far, caprolactam is the most studied lactam and the nylon 6 prepared by this route compares favorably in properties with that prepared by conventional hydrolytic polymerization.

Most of the work reported in the literature employs sodium lactamate salt as catalyst and isocyanate/lactam adducts as initiator. Gabbert and Hedrick [14] preferred to work with acyllactam as the initiator and Grignard salts of caprolactam as the catalyst in view of their ease of handling and fewer side reactions compared with the sodium lactamate and isocyanate system.

Anionic ring opening polymerization of caprolactam (as in other lactams) follows an activated monomer mechanism rather than a conventional activated chain end mechanism. That is, the chain growth reaction proceeds by the interaction of an activated monomer (lactam anion) with the growing chain end (N-acylated chain end in this case). In fact, the anionic attack constitutes the rate-determining step in the propagation. The other characteristic of this mechanism is that activated monomer is regenerated after every unit growth reaction. A typical reaction path for the polymerization of caprolactam is shown in Figure 1.9.

Nucleophilic attack by the amide anion can occur at either the exocyclic or endocyclic carbonyl. The former regenerates the lactamate anion, whereas the latter results in polymerization. Although the locus of nucleophilic attack has no major effects in a homopolymerization, it can exert considerable control over the copolymerizations and on copolymer structure.

From the scheme in Figure 1.9, it is also apparent that the propagation of anionic polymerization requires two active species: lactam anion and N-acyllactam end group. Because the monomer is only consumed via its anion, it is imperative that a certain level of basicity is maintained in the polymerization mixture. The basicity is generally achieved by replacing the proton of the monomer by a less acidic cation such as MgBr+. A large number of catalysts have been reported in the literature, including alkali metals [14,32–34], alkali metal hydroxides [32,35–37], alcoholates [38], carbonates [12,39], Grignard reagents [40], alkylaluminums [41], alkalialuminum hydrides [42] and their partial or total alkoxides [43–45] or their lactam salts [46], quaternary ammonium salts of lactams [47] or of other compounds [48–52], and guanidinium salts of lactams [53].

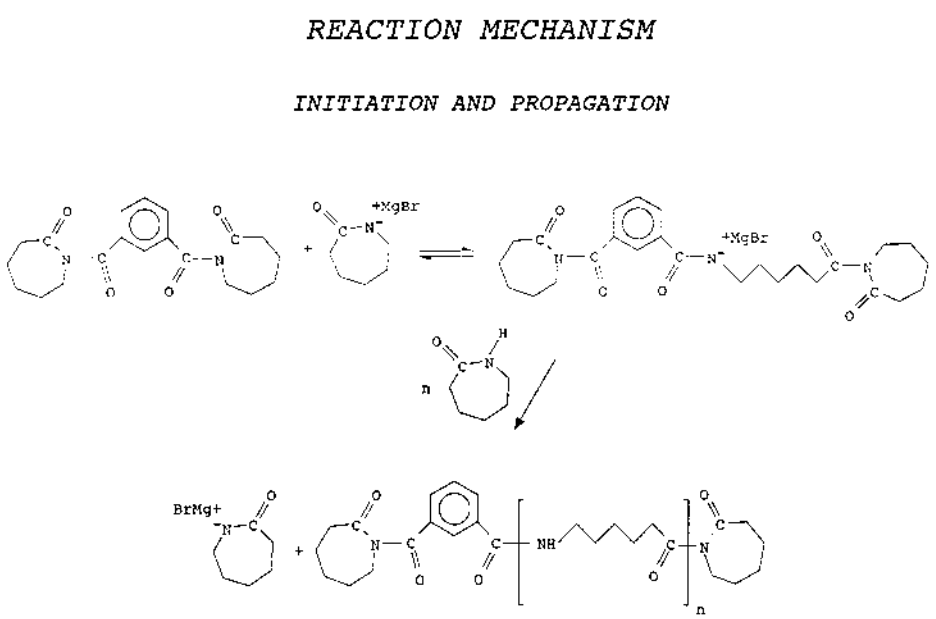


Figure 1.9 Mechanism of anionic polymerization of caprolactam

The anionic catalysts listed earlier react with lactam monomer to first form the salt, which in turn will dissociate to the active species, namely, the lactam anion. A strongly dissociating catalyst in low concentrations, therefore, is always preferable to weakly dissociating catalysts in higher concentrations. The catalytic activity of the various alkali metal and quaternary salts of a lactam generally follows the extent of their ionic dissociation that is controlled by the cation. Activity of a salt decreases with increasing size of the cation due to restricted mobility and decreased ionization potential.

Among the various catalyst systems described earlier, the alkali metal (sodium) lactamate is perhaps the most widely reported in the literature. The Grignard system (caprolactam–magnesium–bromide), despite its many advantages like ease in handling and less acidic MgBr+ cation, has received much less attention. Other catalyst systems may have equal or better reactivity than do the Grignard systems, but they have not been examined at Monsanto to the same extent as the Grignard. Two of the catalyst systems that have received continued investigation outside Monsanto [54] are complexes derived from caprolactam–magnesium–bromide and aluminum alkyls combined with the quaternary salts of lactams, which are often referred to as the *onium salts*. Results to date are quite inconclusive to claim that these systems have a definite advantage over the Grignard.

As initiators, the N-acyllactams have proved to be the most efficient among those investigated by far. Acyllactam end groups in a growing chain, which contain an imide linkage, possess strong acylating power, especially when it involves an already strong nucleophile in a lactam anion. N-acyllactams are generally prepared by the reaction of a lactam with either an anhydride, acid chloride, or an isocyanate. By and large, most of the

work reported in the literature is based on monofunctional initiators, although, in principle, multifunctional initiators can be employed. Initiators with functionality higher than 2 can be expected to produce branched polymers.

The effect of the type and level of initiator on polymerization time, monomer conversion, and polymer molecular weight, the effect of polymerization temperature on the crystallization behavior of the polyamide generated, and the role of a higher lactam like laurolactam on the moisture absorption characteristics of the copolymers are discussed in our previous publication [23].

## 1.3 Kinetics of Anionic Polymerization of Caprolactam

The remainder of this chapter focuses on the kinetics and rheology of the ring opening polymerization of caprolactam to nylon 6. Furthermore, we will discuss the application of rheo-kinetics models to composite processing.

Although a large number of initiators are described in the literature [55,56] to polymerize caprolactam anionically, the primary choice of the catalyst has been sodium (Na), except in the studies at the Monsanto Company by Gabbert and Hedrick [14], Greenley et al. [57], and by us [23–25]. In these studies at Monsanto, caprolactam-magnesium-bromide and isophthaloyl-bis-caprolactam were used as the catalyst and initiator for several reasons, such as the stability and ease of handling of caprolactam-magnesium-bromide compared with sodium, and the proven efficiency of isophthaloyl-bis-caprolactam in earlier studies at the Monsanto Company. The catalyst/initiator combinations used in prior published kinetic studies are: Na/tetraacetyl hexamethylene diisocyanate [58], Na/N-acetylcaprolactam [57,59–62], Na/hexamethylene-1,6-bis-carbamidocaprolactam [62–64], Na/phenyliso-cyanate [57,61,64,65], Na/toluenediisocyanate [61], Na/1,4-diphenylmethanediisocyanate [61], Na/triphenylmethanediisocyanate [61], Na/trimer of toluene diisocyanate [61], Na/phenylcarbamoyl caprolactam [62], Na/2,4-toluene-bis-carbamoyl caprolactam [62], Na/4,4-diphenylmethane-bis-carbamoyl caprolactam [62], Na/hexamethylene-bis-carbamoyl caprolactam [62], and caprolactam-magnesium-bromide/N-acetylcaprolactam [57].

### 1.3.1 Kinetics Model

The reaction mechanism of ring opening homopolymerization of caprolactam consists primarily of two transacylation reactions: initiation and propagation. The initiation occurs by the addition reaction between initiator and catalyst (described in Sec. 1.2). The propagation then occurs by repeating the addition and hydrogen extraction reactions. According to Sebenda [55], such a "regular" reaction scheme is presented "for the sake of simplicity." In reality, deactivation, branching, and a series of reversible transacylation reactions occurring during the anionic ring opening polymerization of caprolactam produce

side reaction products, heterogeneities in the resultant polymer structure, and a broad molecular weight distribution [55].

The low temperature ($\sim$140°C) anionic ring opening polymerization is further complicated by the crystallinity in nylon 6. Magill [66] has reported that the temperature for maximum crystallization rate in nylon 6 is about 140–145°C. The nucleation rate is low above 145°C, whereas viscous effects hinder crystal growth below this temperature. As a result, at about 140–145°C, heterogeneous reaction conditions can be encountered (as we have seen in our studies) if there is simultaneous polymerization of caprolactam and crystallization of the nylon 6 formed.

The phenomenological kinetics of the isophthaloyl-bis-caprolactam–initiated anionic polymerization of caprolactam was obtained by the adiabatic reactor method. Adiabatic polymerization was conducted in a heavily insulated, 250 ml glass beaker (Fig. 1.10) that was set up in an air-circulating oven. The front door of the oven had two hand-holes, similar to a glove box, for inserting the experimenter's hands into the oven. This enabled the catalyst and initiator solutions to be combined, vigorously stirred, and poured into the reaction vessel by working through the two hand-holes without opening the oven. The glass polymerization vessel and the catalyst and initiator solutions in caprolactam were preheated to the initial reaction temperature in the oven. After pouring the mixture of the catalyst and initiator solutions into the beaker, a lid with a copper-constantan thermocouple (Fig. 1.10) was placed on the beaker. The total time for mixing and pouring the catalyst and initiator solutions and covering the beaker with the lid was minimized to less than a couple of seconds. The temperature of the oven as well as inside of the glass polymerization vessel were continually monitored and stored by a data acquisition equipment described in Reference [23]. The samples remained in the adiabatic reactor for at least 30 minutes to insure complete reaction and crystallization.

Principles of the adiabatic reactor method have been discussed elsewhere [67,68]. Under adiabatic conditions, assuming constant heat capacity, constant heat of reaction, and homogeneous reaction, temperature rise data yields fractional conversion, $X$ [68]:

$$X = \frac{[M]_0 - [M]}{[M]_0} = \frac{H}{H_{\text{tot}}} = \frac{(T - T_0)}{(T_f - T_0)} \tag{1.2}$$

The terms in Equation 1.2 are described in Nomenclature. The condition of constant heat capacity can be relaxed if accurate data is available for heat capacity as a function of both conversion and temperature.

In the past, two approaches to kinetic modeling have been used: mechanistic models [57–59,63,65,69] and overall models [60–62,64]. The mechanistic models have attempted to account for each possible reaction individually. Although propagation reactions in caprolactam polymerization consist of only a few types of transacylation reactions, their detailed mechanism, as well as kinetics, are not well understood [55]. In seeking a better kinetic model capable of describing the polymerization process and reflecting the chemistry as well, Cimini and Sundberg [69] modified a rate equation originally derived mechanistically by Reimschuessel [70]. Provaznik et al. [71] have subsequently shown the fundamental importance of changes of the reaction medium on the individual polymerization reactions. As a result appropriate corrections concerning the detailed reaction mechanism and kinetics

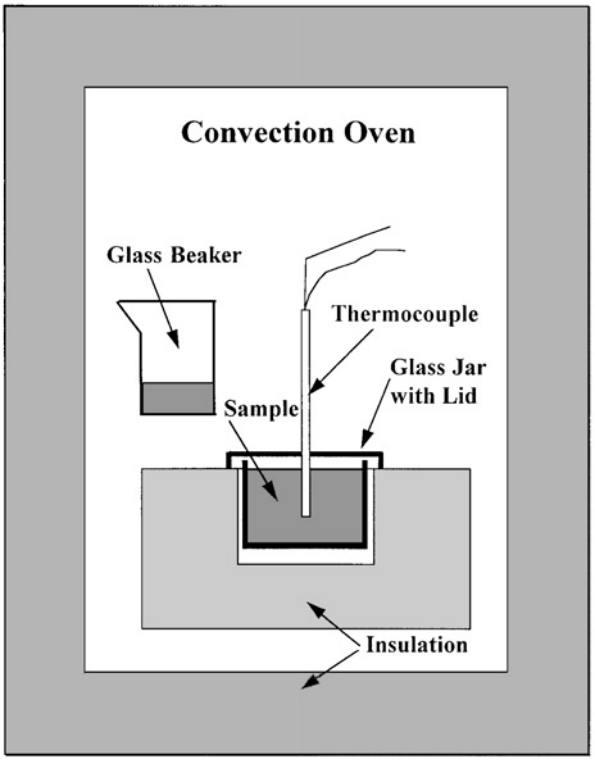


Figure 1.10 Apparatus for measurement of adiabatic temperature rise during anionic polymerization of nylon 6

can be expected in the future; however, the mechanistic models have so far had a limited success in predicting the anionic ring opening polymerization of caprolactam. This approach has been found to be severely hindered by the complex nature of this anionic ring opening polymerization. Although mechanistic models are highly desirable, in the absence of accurate information about the intermediate steps and the possibilities of side reactions like catalyst deactivation and branching, these models are complicated and impractical. On the other hand, the overall models lump all reactions into a single reaction step that accounts for the overall reaction profile like the initial rise in the reaction rate with conversion followed by a decrease in the reaction rate.

We have used an autocatalytic model originally proposed by Malkin et al. [62]. Bolgov et al. [61] found that the originally proposed autocatalytic model [62], which was valid for equal concentration of initiator and catalyst during the anionic polymerization of caprolactam, can be modified for unequal concentration of the initiator and catalyst by an autocatalytic equation of type

$$\frac{dX}{dT} = k \exp\left(\frac{U}{RT}\right) \frac{[A][C]}{[M_0]} (1 - X) \left\{ 1 + \frac{b}{([A][C])^{1/2}} X \right\} \tag{1.3}$$

The terms in Equation 1.3 (Malkin's autocatalytic model) are described in Nomenclature. In Malkin's autocatalytic model, the concentration of the activator, [*A*], is defined as the concentration of the initiator times the functionality of the initiator. For a difunctional initiator [e.g., isophthaloyl-bis-caprolactam, the concentration of the activator (acyllactam) is twice the concentration of the initiator]. The term [*C*] is defined as the concentration of the metal ion that catalyzes the anionic polymerization of caprolactam. In a magnesium-bromide catalyzed system, the concentration of the metal ion is the same as the concentration of the caprolactam-magnesium-bromide (catalyst) because the latter is monofunctional.

Malkin's autocatalytic model is an extension of the first-order reaction to account for the rapid rise in reaction rate with conversion. Equation 1.3 does not obey any mechanistic model because it was derived by an empirical approach of fitting the calorimetric data to the rate equation such that the deviations between the experimental data and the predicted data are minimized. The model, however, both gives a good fit to the experimental data and yields a single pre-exponential factor (also called the *front* factor [64]), *k*, activation energy, *U*, and autocatalytic term, *b*. The value of the front factor *k* allows a comparison of the efficiency of various initiators in the initial polymerization of caprolactam [62]. On the other hand, the value of the autocatalytic term, *b*, describes the intensity of the self-acceleration effect during chain growth [62].

### 1.3.2 Kinetic Model Verification

In our studies, the catalyst and initiator system was comprised of caprolactam-magnesium-bromide and isophthaloyl-bis-caprolactam, respectively. We determined the optimum values of the kinetic parameters in Malkin's autocatalytic model (Eq. 1.3), which consist of *k*, *U*, and *b*, by regression analysis.

Equation 1.3 was linearized by transposing $(1 - x)$ and the autocatalytic term to the left and then taking the logarithms of both sides of the equation. Fixing the value of *b*, a linear regression was performed for *k* and *U*. This procedure was repeated for several values of *b*, and an optimum value of *b* was chosen that gave the best fit straight line to the linearized equation. The corresponding values of *k* and *U* obtained from the best fit straight line were chosen as the optimum.

The values of the activation energy *U,* the front factor *k*, and the autocatalytic term *b* for the caprolactam-magnesium-bromide/isophthaloyl-bis-caprolactam system, as well as other catalyst/initiator systems, are shown in Table 1.2. The values of the kinetic constants for the caprolactam-magnesium-bromide/isophthaloyl-bis-caprolactam system are based on the adiabatic temperature rise data in Figure 1.11, with initial polymerization temperatures of 117 and 136°C. It is important to note that the activation energy of the magnesium-catalyzed system is considerably lower (30.2 kJ/mol vs. about 70 kJ/mol) than that for the sodium catalyzed system [60,64]. This is because the magnesium cation is less electropositive than the sodium cation. Compared with the sodium cation, the magnesium cation is therefore less tightly bound to the caprolactam anion.

In the only other reported study on the kinetics of anionic ring opening homopolymerization of caprolactam using caprolactam-magnesium-bromide, Greenley et al. [57]

**Table 1.2 Kinetic Constants for Anionic Polymerization of Caprolactam with Different Catalyst and Initiator Systems**

| System (catalyst/initiator) | Source | Model | Analytical method | U (kJ/mol) | k (L/mol s) | b (L/mol) |
|---|---|---|---|---|---|---|
| MgBr+/IBT[(a)] | Davé et al. [24] | Malkin's autocatalytic model | Adiabatic temperature analyzed by regression analysis | 30.2 | $1.49 \times 10^4$ | 2.17 |
| Na/HMCCl[(b)] | Malkin et al. [60] | Same as above | Same as above | $63 \pm 6$ | $4.17 \times 10^8$ | 0.066 |
| Na/HMCCl[(b)] | Sibal et al. [64] | Same as above | Same as above | $63.8 \pm 0.5$ | $2.23 \times 10^8$ | $1.15 \pm 0.5$ |
| MgBr+/NAC[(c)] | Greenley et al. [57] | Greenley's mechanistic model | Assuming pseudo first-order, isothermal reaction during low conversion | 46 | N/A | N/A |
| MgBr+/IBT[(a)] | Davé et al. [24] | First-order rate dependence on monomer concentration | Same as above | 40.6 | $7.62 \times 10^5$ | N/A |

[(a)] = Magnesium-bromide-caprolactam/isophthaloyl-bis-caprolactam
[(b)] = Sodium/hexamethylene-1,6,-bis-carbamidocaprolactam
[(c)] = Magnesium-bromide-caprolactam/N Acetylcaprolactam
N/A = Not available or not applicable.

[Refs. on p. 29]

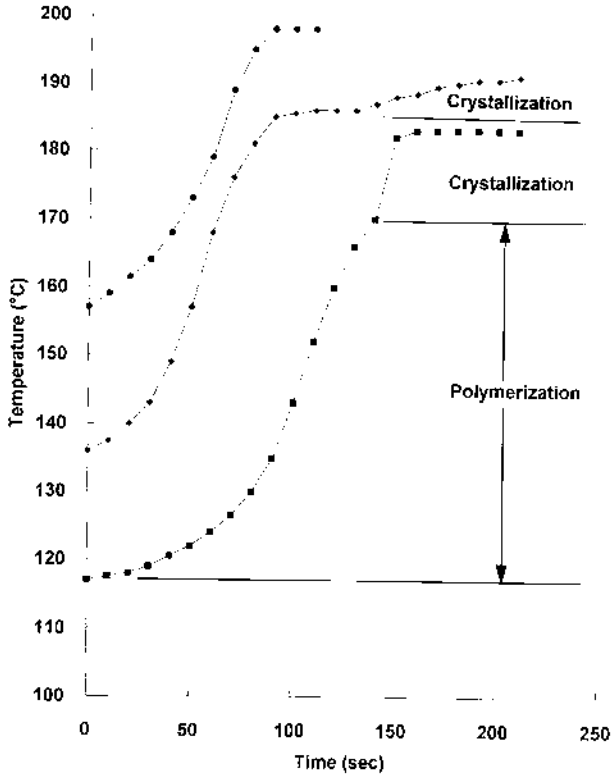


Figure 1.11 Adiabatic conversion of nylon 6: Experimental data for initial polymerization temperatures of 117°C (bottom line), 136°C (middle line), and 157°C (top line) with acyllactam and caprolactam-magnesium-bromide concentrations of 70 and 108 mmol/L, respectively

determined the value of the activation energy by making the following assumptions: (1) the reaction is pseudo–first-order; (2) the reaction is isothermal—consequently, their experimental data were below 20 percent conversion due to the need for pseudoisothermal conditions, and (3) there is a half-order dependence on the initial catalyst concentration. The third assumption was made in the derivation of the rate equation to obtain a better fit. In addition, their rate equation was derived by considering an irreversible degradation reaction with a rate constant $k_d$ in addition to the polymerization reaction with a rate constant, $k_p$. The degradation rate constant, however, was found to be negligible—$k_p$ was approximately 1500 times larger than $k_d$ [57].

The role of the isothermal and pseudo–first-order reaction assumptions on the observed value of activation energy was assessed to allow comparison of our data to previous work by modifying Malkin's autocatalytic equation so that the autocatalytic term $b$ is equal to zero. The values of the activation energy and front factor were calculated using short-time, low-conversion data. By making the autocatalytic term equal to zero, the modified Malkin autocatalytic model becomes a first-order rate reaction. Table 1.2 shows that by assuming a

pseudo–first-order, isothermal reaction during low conversion, the values of the activation energy for the caprolactam-magnesium-bromide catalyzed ring opening homopolymerization of caprolactam are calculated to be nearly the same for Greenley et al. [57] and for us (46 kJ/mol vs. 40.6 kJ/mol). As a matter of fact, even the value of the activation energy calculated by Greenley et al. [57] for the sodium/N-acetylcaprolactam system assuming pseudo–first-order, isothermal reaction during low conversion is much larger than the activation energy reported by other investigators [59–61] for the same catalyst/initiator system (92 kJ/mol vs. about 70 kJ/mol). Based on the preceding calculations, the implication of assuming a pseudo–first-order reaction (i.e., neglecting the autocatalytic term and using only the low conversion data in the determination of the activation energy) is likely to result in gross overprediction in the value of the activation energy.

It appears that most activation energy values in the literature for sodium catalyzed anionic ring opening homopolymerization of caprolactam are in the range of 63–71 kJ/mol despite the variety of initiators used [58–6,64]. This indicates that the value of the activation energy is probably independent of the initiator used and dependent only on the catalyst used in the anionic ring opening polymerization of caprolactam. The results of this study, as well as the study by Greenley et al. [57], add further credence to the last statement that the activation values for a caprolactam-magnesium-bromide catalyzed system is much lower than the activation energy values for a sodium catalyzed system (30 kJ/mol versus about 70 kJ/mol).

We calculated the values of $U$, $k$, and $b$ for caprolactam-magnesium-bromide/isophthaloyl-bis-caprolactam system to be 30.2 kJ/mol, $1.49 \times 10^4$ L/mol, and 2.17 L/mol, respectively. We have used these optimized values for comparing model predictions with experimental data obtained from adiabatic polymerization to study the effect of initial polymerization temperature and effects of initiator and catalyst concentrations [24].

## 1.4 Viscosity Growth During Anionic Polymerization of Caprolactam

In order to understand the time-dependent growth of complex viscosity, $|\eta^*|$, during the anionic polymerization of caprolactam, we have developed a concurrent polymerization and rheological test methodology. In this test, two monomer streams — one containing catalyst and the other containing initiator — are mixed essentially instantaneously as they enter the gap between the parallel plates in a Rheometrics Mechanical Spectrometer. The polymerization is thus carried out under isothermal conditions, over the range of 120–160°C, while rheological measurements are made. The complex viscosity $|\eta^*|$ was monitored with an end toward defining the rheokinetics of the anionic ring opening homopolymerization of caprolactam using isophthaloyl-bis-caprolactam and caprolactam-magnesium-bromide as initiator and catalyst. Isothermal rheometry at five temperatures was accomplished for one initiator/catalyst concentration with the objectives of: (1) to define the rheology of nylon 6 anionically

polymerizing by ring opening polymerization in caprolactam; and (2) to correlate this rheology with the kinetics of polymerization.

### 1.4.1 Viscosity Model

The following relation was used for determining the complex viscosity of the polymerizing system [64]:

$$|\eta^*| = |\eta_0| \exp(k^* X) \tag{1.4}$$

where $|\eta^*|$ is the complex viscosity of nylon 6 anionically polymerizing in its monomer, $|\eta_0|$ is the complex viscosity of caprolactam monomer, $k^*$ is a constant, and $X$ is fractional conversion. The complex viscosity of the monomer, $|\eta_0|$ follows an Arrhenius temperature dependence [64]

$$|\eta_0|(T) = 2.7 \times 10^{-7} \exp(3525/T) \quad \text{(Pa s)} \tag{1.5}$$

### 1.4.2 Viscosity Model Verification

Complex viscosity growth during anionic polymerization of caprolactam was measured under isothermal conditions using a Rheometics Dynamic Mechanical Analyzer (DMA), RMS-800. Figure 1.12 shows a schematic diagram of the delivery method for simultaneously injecting two streams through a static mixer into the rheometer platen gap, which is where the polymerization reaction and oscillatory complex viscosity measurement occur simultaneously. Prior to injection of a sample, the instrument was first equilibrated at the desired temperature and the gap was set. The details of the instrument and run conditions are given in Reference [25].

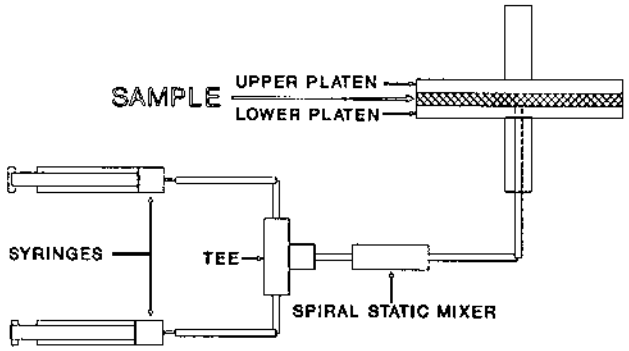


Figure 1.12 Dual stream injection system for in situ rheokinetic study of anionic ring opening polymerization of caprolactam

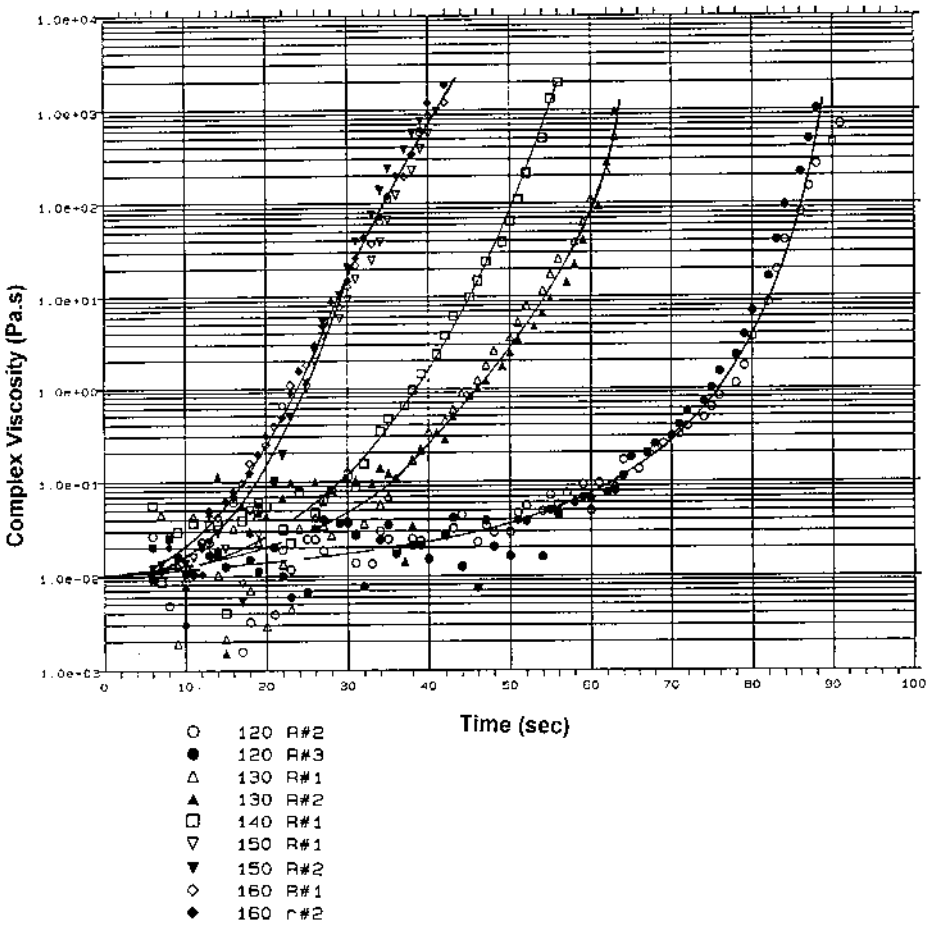


Figure 1.13 Isothermal complex viscosity rise during anionic polymerization of caprolactam using caprolactam-magnesium-bromide/isophthaloyl-bis-caprolactam as the catalyst/initiator system. Run numbers and polymerization temperatures are shown in the legend

The single feed composition investigated consisted of 133 mmols/L of caprolactam-magnesium-bromide and 45 mmols/L of the difunctional isophthaloyl-bis-caprolactam. Note that 45 mmols/L of the difunctional isophthaloyl-bis-caprolactam contain 90 mmols/L of the active acyllactam group, which react with the monofunctional caprolactam-magnesium-bromide to initiate the polymerization reaction.

Upon mixing and injection of the caprolactam monomer streams into the rheological instrument, polymerization was initiated and continued, whereas simultaneously monitoring the complex viscosity and other rheological parameters of the polymerizing system. The maximum measurable complex viscosity levels were achieved in about 100 s or less, depending on temperature.

At each temperature, the expected rapid rise of complex viscosity with conversion, molecular weight build-up, and ultimate solidification was observed and the complex

viscosity–time relationship was quantified. The time to achieve maximum permissible torque on the instrument ranged from about 90 s at 120°C to 40 s at 160°C. This corresponds to $10^3$ Pa s ($10^4$ poise) for the geometry used and is on such a steep slope of the complex viscosity–time curve that it is very close to the time for near infinite complex viscosity (i.e., total solidification).

Figure 1.13 shows replicated complex viscosity–time curves for all five temperatures. Some difficulty in reproducibly filling the gap between the parallel plates was encountered, leading to the requirement of measurement replication and averaging of results. In addition, the initial (very early time) viscosities were about 0.01 Pa s (ten times that of water) and are outside the sensitivity range of the instrument, leading to very large scatter at low times. These caveats notwithstanding, the data is relatively good, and provided a quantitative basis for modeling the matrix viscoelastic build-up during the reaction injection pultrusion process.

Figure 1.14 shows time to achieve a given complex viscosity as a function of polymerization temperature. These curves are fitted with a quadratic equation (second-order polynomial).

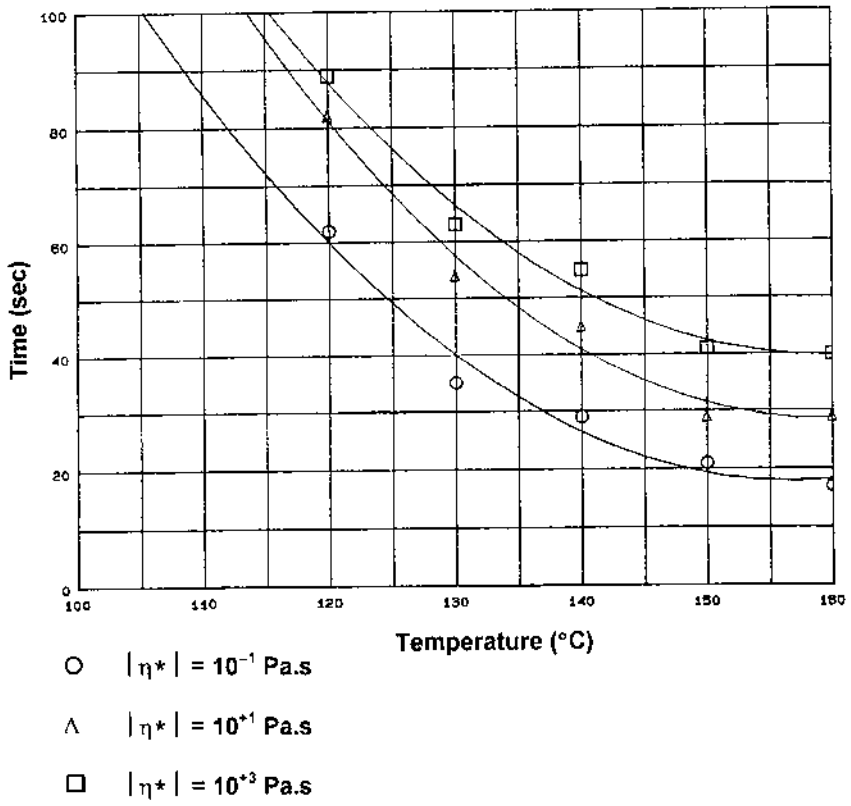


Figure 1.14 Time to reach complex viscosity of 0.1, 10, and 1000 Pa s as a function of temperature during anionic polymerization of caprolactam using caprolactam-magnesium-bromide/isophthaloyl-bis-caprolactam as the catalyst/initiator system. Complex viscosity is shown in the legend

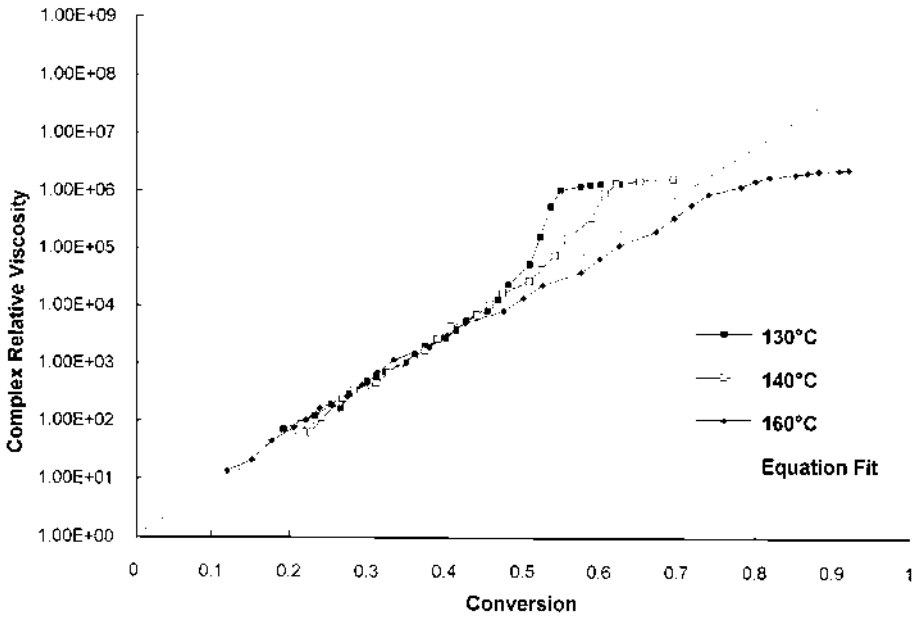


Figure 1.15 Relative complex viscosity ($|\eta^*|/|\eta_0|$) versus calculated conversion for polymerization at 130, 140, and 160°C. Phenomenological equation to fit the data prior to gelation is also shown

Figure 1.15 shows relative complex viscosity ($|\eta^*|/|\eta_0|$) as a function of conversion at 130, 140, and 160°C. Conversion was calculated by the kinetic model described previously [24]. Figure 1.15 shows that between 130 and 160°C (except 150°C) all curves are nearly identical below 50 percent conversion. For polymerization at 130 and 140°C, a sharp increase in relative complex viscosity was observed beyond 50 percent conversion. Sibal et al. [64] suggest that the sharp increase in relative complex viscosity during anionic ring opening polymerization of caprolactam is due to physical "gelation" that probably results from mechanical interlocking of the crystallites being formed during polymerization. This effect is likely not gelation, but simply the result of rigid crystallites on viscosity. The conversion at which the relative complex viscosity curve deviates from the linear, straight-line fit depends on the polymerization temperature because both kinetics of polymerization and kinetics of crystallization are temperature dependent. For polymerization near 145°C, where the crystallization rate is greatest [64], crystallization kinetics strongly competes with chemical kinetics. On the other hand, for polymerization at 160°C, crystallization rate is drastically reduced [66] and, therefore, the 160°C curve does not exhibit the gelation effect.

Even though a mechanistic explanation of the complex viscosity rise and gelation is not available at this time, the information in Figure 1.15 is useful in understanding and modeling reaction injection molding, reaction injection pultrusion, and other fiber-reinforced composite processes that are based on anionic ring opening polymerization of caprolactam. Below

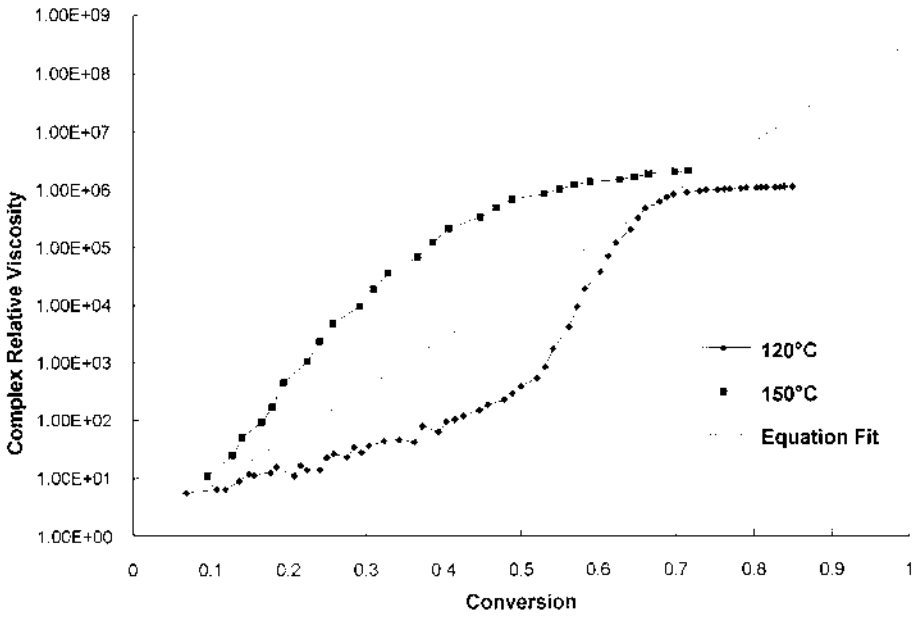


Figure 1.16 Relative complex viscosity ($|\eta^*|/|\eta_0|$) versus calculated conversion for polymerization at 120 and 150°C. Linear, straight-line fit to the phenomenological equation $|\eta^*|/|\eta_0| = \exp(19.6\ X)$ is also shown

50 percent conversion all the curves are almost linear, which suggests a phenomenological equation of the form:

$$|\eta^*|/|\eta_0| = \exp(19.6X) \quad \text{for } X < 0.5 \tag{1.6}$$

where 19.6 is the constant that defines the relative complex viscosity rise during anionic ring opening polymerization of caprolactam using caprolactam-magnesium-bromide/isophthaloyl-bis-caprolactam as the catalyst/initiator system. In Equation 1.6, the temperature dependence of $|\eta^*|$ is that for $|\eta_0|$ defined in Equation 1.5.

For sodium/hexamethylene-1,6-bis-carbamidocaprolactam system, Sibal et al. [64] found the value of the constant $k^*$ in Equation 1.4 to be 17.5. Note that the values of the constant $k^*$ in Equation 1.4 that defines the relative complex viscosity rise during anionic ring opening polymerization of caprolactam are comparable for both caprolactam-magnesium-bromide/isophthaloyl-bis-caprolactam and sodium/hexamethylene-1,6-bis-carbamidocaprolactam as the catalyst/initiator systems even though the kinetic constants for anionic polymerization for these systems are extremely different (see Table 1.2).

Figure 1.16 shows the relative complex viscosity as a function of conversion at 120 and 150°C. The 150°C curve shows a dramatic rise due to the simultaneous crystallization during polymerization. In addition, notice in Figure 1.13 that the complex viscosity–time curves of 150 and 160°C polymerization tend to converge. Both these effects—the nonlinear rise in relative complex viscosity in Figure 1.16 and the convergence of 150 and 160°C curves in

Figure 1.13—occur because of simultaneous crystallization and polymerization at 150°C. This temperature is near the maximum crystallization rate temperature (~145°C) of nylon 6 homopolymer [66]. The presence of solid crystallites increases the complex viscosity of the polymerizing system because of a filler effect.

In Figure 1.16, the 120°C curve deviates from the straight line at a conversion of about 10 percent. This effect is due to "sluggish" polymerization at 120°C like that we have observed in our kinetics study (see Figure 1.5a in Ref. 24). The predicted conversion ($x$-axis values in Figure 1.16) is based on Malkin's autocatalytic phenomenological model that does not account for either crystallization or diffusion-controlled kinetics. In Figure 1.16, however, the polymerization at 120°C becomes diffusion controlled after about 10 percent conversion. The predicted values of conversion by Malkin's autocatalytic rate equation, therefore, are overestimated values of the true conversion resulting from diffusion controlled kinetics. This error results in the nonlinearity of the 120°C curve.

As a final note, we question why the relative complex viscosity versus conversion curve for the 140°C polymerization did not deviate (up to 50 percent conversion) from the straight-line fit even though Magill's data on crystallization rate of hydrolytic nylon 6 (i.e., nylon 6 made by the conventional, hydrolytic process) versus temperature shows a maximum in the crystallization rate at about 140–145°C. One possibility is that nylon 6 formed by anionic polymerization below the melting point of nylon 6 is a mixture of two crystalline structures: $\alpha$ and $\gamma$ (see Ref. [23]). The melting points of $\alpha$ and $\gamma$ structures are about 256 and 228°C, respectively [72]. For anionically formed nylon 6 that is a mixture of $\alpha$ and $\gamma$ structures, the temperature for maximum crystallization may be higher than the temperature for maximum crystallization of hydrolytic nylon 6 ($\gamma$ structure). Because Magill's data were obtained on hydrolytic nylon 6, these data may not be directly applicable to the crystallization of nylon 6 polymerizing in molten caprolactam during anionic ring opening polymerization of caprolactam.

## 1.5 Application of Rheo-Kinetics Modeling to Reaction Injection Pultrusion

Reactive injection pultrusion (RIP) is a means of applying the thermoset pultrusion process, with appropriate changes, to thermoplastic systems. In RIP, glass fibers are pulled through a "feed zone" where the caprolactam monomer, along with catalyst and initiator, are injected. The low viscosity monomers exhibit excellent fiber wetting in the feed zone, and then polymerize around the fibers in the die at 130–200°C. A puller, located beyond the die, pulls the glass fiber reinforced nylon 6 composite. A typical composition of the glass fiber/nylon 6 pultruded composite is 75 percent glass and 25 percent nylon 6, by weight. The typical pultrusion line speed is 1–2 m/min. Figure 1.17 is a schematic of the reaction injection process.

In this section, we will describe the application of the rheokinetic model to adiabatic and isothermal pultrusion by the RIP process. Adiabatic pultrusion is defined as a pultrusion

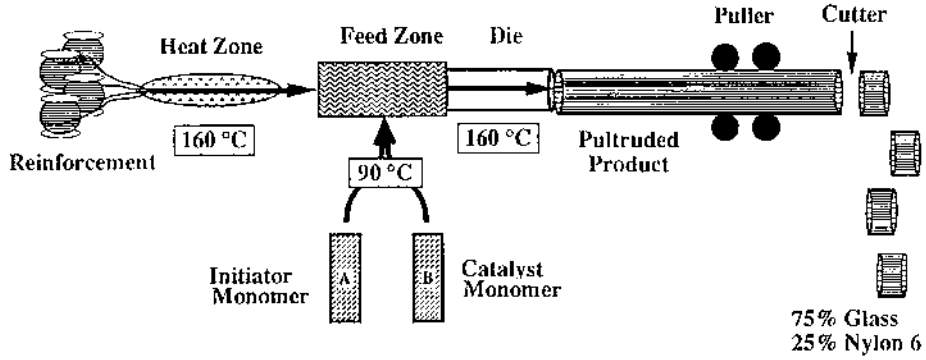


Figure 1.17 Schematic of the reactive pultrusion process

process where no heat transfer occurs across the boundaries (surface) of the pultrudate in the die. On the other hand, an isothermal pultrusion is a pultrusion process where the temperature of the pultrudate is maintained constant from the entrance to the exit of the die. During adiabatic pultrusion, the heat of polymerization, if any, is absorbed by the pultrudate, and the absorbed heat causes the temperature of the pultrudate to increase. In reality, adiabatic and isothermal pultrusion are just hypothetical concepts. In practice, near adiabatic pultrusion conditions can be achieved by maintaining the die wall temperature as close as possible to the predicted temperature of the pultrudate for adiabatic pultrusion. Because RIP of glass fiber nylon 6 is an exothermic process, isothermal operation would require extraction of heat from the die as conversion proceeds. Isothermal pultrusion is impractical because it is very difficult to maintain a constant pultrudate temperature throughout the die. Despite these limitations, modeling adiabatic and isothermal pultrusion processes is extremely valuable in providing insight into the process and to discriminate between weak and strong factors that affect the pultrusion process. There are two alternatives to the preceding approach: (1) Develop an experimental design strategy and conduct experiments to determine the process conditions; (2) Model a real-life pultrusion process. Both of these approaches, however, have major drawbacks. The former approach is expensive and time consuming, whereas the latter approach is tedious because it requires modeling of simultaneous heat, mass, and momentum transfer along with chemical reaction in a multiphase system. In order to simplify the modeling, yet obtain germane information, we have modeled adiabatic and isothermal pultrusion. The adiabatic and isothermal pultrusion models finally reduce to the rheo-kinetics of the matrix resin in the presence of the fiber.

Pultrusion is a steady-state process in which the fiber–resin mass changes its properties as it moves from the entrance to the exit of the die. In order to track the temperature, polymer conversion, and other properties of the fiber–resin mass as it moves along the die, it is useful to define a *representative volume element* (RVE) that rides along the fiber at the line speed of the pultrusion process. An RVE is defined such that it will contain *both* the solid phase (i.e., fibers and resin), irrespective of its location in the composite. In real-life pultrusion, a thermocouple wire that passes through the pultrusion die tracks the temperature of an RVE in the composite.

In the present pultrusion modeling study, the composition of the glass fiber/nylon 6 pultrudate was chosen as 75 percent glass and 25 percent nylon 6 by weight. In addition, the single-feed composition investigated consisted of 108 mmols/L of caprolactam-magnesium-bromide and 35 mmols/L of the difunctional isophthaloyl-bis-caprolactam (i.e., 70 mmols/L of the active acyllactam group), and we performed a parametric study on an adiabatic pultrusion process by changing the following variables:

1. temperature of the incoming glass fiber
2. temperature of the caprolactam monomer feed

In addition, we also compared the effect of adiabatic versus isothermal processing on polymerization time.

Figure 1.18 shows the calculated temperature of an RVE during adiabatic pultrusion as a function of the temperature of the incoming glass fiber when the temperature of the incoming caprolactam monomer is 90°C. At time $t = 0$, the RVE is located at the point of injection of the monomer into the die. In addition, at time $t = 0$, the initial polymerization temperature (IPT) is the average of the incoming glass fiber and monomer temperatures, determined by the rule of mixtures by weight:

$$T_0 = \frac{(1 - w_f)Cp_{\text{caprolactam}}T_{0\text{caprolactam}} + w_f Cp_{\text{fiber}}T_{0\text{fiber}}}{(1 - w_f)Cp_{\text{caprolactam}} + w_f Cp_{\text{fiber}}} \tag{1.7}$$

where $T_0$ = initial polymerization temperature, $T_{0\text{caprolactam}}$ = temperature of the incoming caprolactam feed, $T_{0\text{fiber}}$ temperature of the incoming fiber, $w_f$ = weight fraction of the fiber in the composite, $Cp_{\text{caprolactam}}$ = specific heat of caprolactam, and $Cp_{\text{fiber}}$ = specific heat of the fiber.

The specific heat of E glass fiber is 0.192 cal/gm K (i.e., 0.804 J/gm K) [73]. The specific heat of caprolactam as a function of temperature was fitted to the following equation from experimental data available in Monsanto:

$$Cp_{\text{caprolactam}}\ (\text{J/gm K}) = 0.01114T - 1.7057 \tag{1.8}$$

where $T$ is the temperature of caprolactam in K.

In Figure 1.18, we see that as the temperature of the incoming fiber increases from 100 to 160°C, the time for complete conversion decreases from 240 to 150 s. The upper limit of the temperature of the incoming fiber was set at 160°C because the sizing on most of the available glass fibers burns at temperatures higher than 160°C.

A further leverage to increase the reaction rate was to increase the temperature of the incoming caprolactam monomers. Figure 1.19 is similar to Figure 1.18 except that the incoming monomer feed is at 100°C rather than 90°C. Increasing the incoming monomer temperature from 90 to 100°C reduces the time to complete conversion. For example, for the case where the temperature of the incoming fiber was 120°C, the time to complete conversion was reduced from 240 to 210 s. In addition, one should note from Figures 1.18 and 1.19 that the adiabatic temperature rise in the composite with 75 percent glass by weight is only about 30°C, instead of the 50°C rise seen typically during anionic polymerization of caprolactam into unreinforced nylon 6 (see adiabatic temperature rise data in Figure 1.11 with initial polymerization temperatures of 117 and 136°C). The smaller increase in the temperature of the composite as compared with unreinforced nylon 6 is due to the absorption of some of the

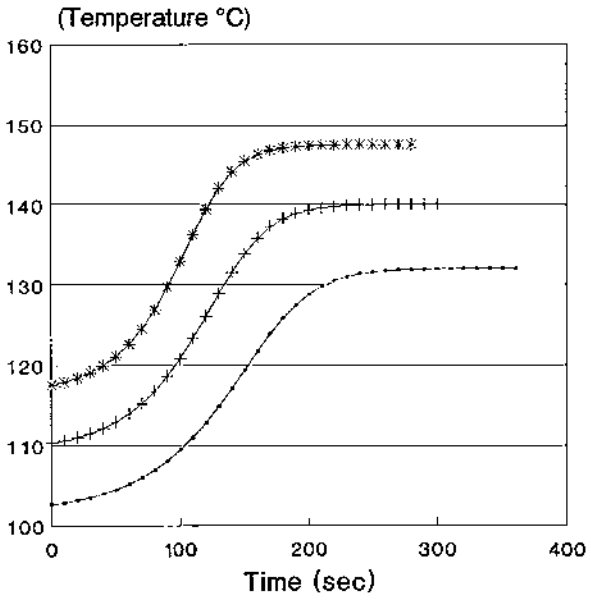


Figure 1.18 The temperature of an RVE during adiabatic pultrusion when the temperature of the incoming caprolactam monomer was 90°C and the temperature of the incoming glass fiber was 120°C (bottom line), 140°C (middle line), and 160°C (top line)

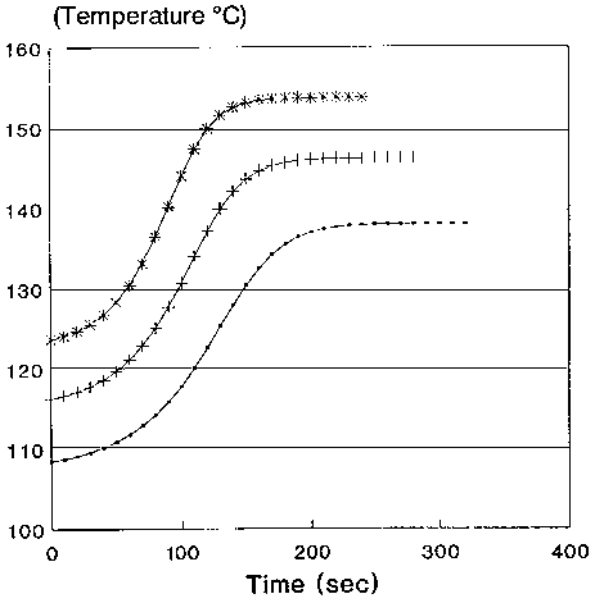


Figure 1.19 The temperature of an RVE during adiabatic pultrusion when the temperature of the incoming caprolactam monomer was 100°C and the temperature of the incoming glass fiber was 120°C (bottom line), 140°C (middle line), and 160°C (top line)

heat of polymerization by the glass to increase the temperature of the glass to that of the reacting monomer surrounding the glass.

Figures 1.20 and 1.21 show calculated conversion as a function of time during adiabatic and isothermal pultrusion of glass fiber/nylon 6 composites with 75 percent glass fiber by weight and monomer feed concentrations stated earlier. The isothermal pultrusion temperature and the initial temperature for adiabatic pultrusion are 136 and 157°C, respectively, in Figures 1.20 and 1.21. Because the adiabatic temperature rise of the composite is about 30°C, the final temperatures are 166 and 187°C, respectively, in Figures 1.20 and 1.21. Figure 1.20 shows that complete conversion (indicated as 1.0, but is about 0.95 in reality) is achieved in 125 and 190 s, respectively, for adiabatic and isothermal processing when initial polymerization temperature was 136°C. Figure 1.21 shows complete conversion times of 90 and 120 s, respectively, for adiabatic and isothermal processing when initial polymerization temperature was 157°C. (Note that in the case of isothermal RIP processing, the polymerization temperature is constant within the full length of the die.) Based on the rheo-kinetic modeling it is clear that the adiabatic pultrusion process is more desirable because the times for complete conversion is shorter than in the case of the isothermal RIP process. The faster conversion by the adiabatic RIP process resulted in increased throughput of the pultruded composite. In addition, it has been our experience that it was extremely difficult to maintain a constant temperature along the full length of the die. On the other hand, we found it relatively easy to set the temperatures along the die to be nearly equal to the adiabatic polymerization temperatures.

From Equation 1.4, the complex viscosity at 57 percent conversion of the caprolactam monomer, which may be defined as solidification or "gel" point, is 100 Pa s (1000 Poise). Combining the information on conversion at the gel point with the data presented in Figures 1.20 and 1.21, the time to gel formation during pultrusion can be estimated.

In a real-life RIP of glass fiber nylon 6, the process is neither isothermal nor adiabatic, as stated earlier. In real-life RIP processes, external heaters are mounted on the die to keep all the exothermic heat within the pultruded product and, sometimes, even add external heat into the pultruded product to enhance the reaction rate further. The adiabatic temperature rise plots shown in this section are valuable tools for determining the minimum temperature along the length of the die and the desired residence time in the die for adiabatic conversion. The pulling speed is, in turn, estimated by dividing the die length by the residence time in the die. The temperature along the die length, however, may be maintained higher than adiabatic conversion temperature for faster processing.

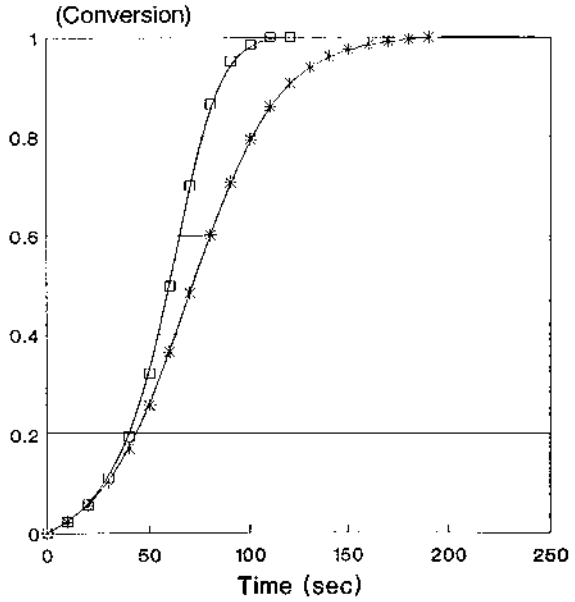


Figure 1.20 Conversion in an RVE during adiabatic (top line) and isothermal (bottom line) pultrusion of glass fiber nylon 6 composite when the initial temperature for adiabatic pultrusion and the isothermal pultrusion temperature were 136°C

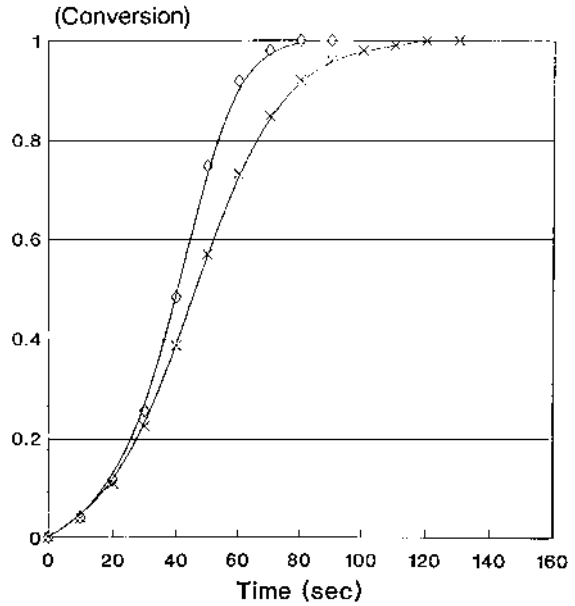


Figure 1.21 Conversion in an RVE during adiabatic (top line) and isothermal (bottom line) pultrusion of glass fiber nylon 6 composite when the initial temperature for adiabatic pultrusion and the isothermal pultrusion temperature were 157°C

## 1.6 Concluding Remarks

This chapter reviewed the chemistry of ring opening polymerization of cyclic monomers that yield thermoplastic polymers of interest in composite processing. In addition, this chapter focuses on the chemistry, kinetics, and rheology of the ring opening polymerization of caprolactam to nylon 6. Finally, these rheokinetics models are applied to the reactive injection pultrusion (RIP) process.

The kinetics of anionic ring opening polymerization of caprolactam initiated by isophthaloyl-bis-caprolactam and catalyzed by caprolactam-magnesium-bromide satisfactorily fit Malkin's autocatalytic model below 50 percent conversion. The calculated value of the overall apparent activation energy for this system is 30.2 kJ/mol versus about 70 kJ/mol for Na/hexamethylene-1,6,-bis-carbamidocaprolactam as the initiator/catalyst system.

The rheokinetics of polycaprolactam polymerizing in the monomer shows that below 50 percent conversion, the relative complex viscosity versus conversion of the nylon 6 homopolymerization is defined by the phenomenological equation $|\eta^*|/|\eta_0| = \exp(19.6\,X)$, where $|\eta^*|$ is the complex viscosity of nylon 6 anionically polymerizing in its monomer, $|\eta_0|$ is the viscosity of caprolactam monomer, and $X$ is fractional conversion.

### Nomenclature

| | |
|---|---|
| $[A]$ | Activator, acyllactam concentration, mol/L |
| $b$ | Autocatalytic term, L/mol |
| $[C]$ | Catalyst, caprolactam-magnesium-bromide, concentration, mol/L |
| $Cp_{\text{caprolactam}}$ | Specific heat of caprolactam, J/gm K |
| $Cp_{\text{fiber}}$ | Specific heat of the fiber, J/gm K |
| $H$ | Heat of polymerization, J/mol |
| $H_{\text{tot}}$ | Total heat of polymerization, J/mol |
| $k$ | Pre-exponential or front factor, L/mol s in Equation 1.3 |
| $k^*$ | Constant in Equation 1.4 |
| $M$ | Monomer concentration, mol/L |
| $M_0$ | Initial monomer concentration, mol/L |
| $R$ | Universal Gas Constant, J/mol K |
| $T$ | Temperature, K |
| $T_0$ | Initial polymerization temperature, K |
| $T_{0\text{caprolactam}}$ | Temperature of the incoming caprolactam feed, K |
| $T_{0\text{fiber}}$ | Temperature of the incoming fiber, K |
| $T_f$ | Final adiabatic temperature, K |
| $t$ | Time, s or sec |
| $U$ | Activation Energy, J/mol |
| $w_f$ | Weight fraction of the fiber in the composite |

| | |
|---|---|
| $X$ | Fractional conversion |
| $\|\eta^*\|$ | Complex viscosity during ring opening polymerization, Pa s |
| $\|\eta_0\|$ | Complex viscosity of the monomer, Pa s |

## Acknowledgments

Financial support and release for publication were provided by Monsanto Company, Plastics Division (sold to Bayer Corporation in 1995). The authors wish to thank the following fine individuals: Robert Mendelson and Donald Williams for guiding the rheological measurements at Monsanto's Physical and Analytical Science Center, Springfield, MA; Lionel Stebbins for doing the kinetics experiments; Allen Padwa for making Figures 1.1–1.8; Kamran Tavangar for making Figure 1.17; and Donald Nardi for operating the reaction injection pultrusion process.

## References

1. Ivin, K.J., Saegusa, T., eds. *Ring Opening Polymerization* (1984) Elsevier Applied Science Publishers, London
2. Frisch, K.C., Reegen, S.L., eds. *Ring Opening Polymerization* (1969) Marcel Dekker, Inc., New York
3. Furukawa, J., Saegusa, T., eds. *Ring Opening Polymerization of Aldehydes and Oxides* (1963) Wiley-Interscience, New York
4. Penczek, S., Kubisa, P., Matyjaszewski, K., *Adv. Polym. Sci.* (1985) 68/69, p. 1
5. Penczek, S., Kubisa, P., Mayjaszewski, K., *Adv. Polym. Sci.* (1980) 37, p. 1
6. Chujo, Y., Saegusa, T., eds. *Encyclopedia of Polymer Science and Engineering* (1988) 14, John Wiley and Sons, New York, p. 622
7. Joyce, R.M., Ritter, D.M., (1941) U.S. Patent 2,251,519
8. Sebenda, J., *J. Macromol. Sci., Chem.* (1972) A6, p. 1145
9. Sebenda, J., *Prog. Polym. Sci.* (1978) 6, p. 123
10. Sebenda, J., *Pure Appl. Chem.* (1976) 48, p. 329
11. Sekiguchi, H., *J. Chem. Soc. Japan* (1967) 88, p. 577
12. Wichterle, O., Sebenda, J., *Collect. Czech. Chem. Communs.* (1956) 21, p. 312
13. Wichterle, O., Sebenda, J., Kralicek, J., *Fortschr. Hochpolym. Forsch.* (1961) 2, p. 578
14. Gabbert, J.D., Hedrick, R.M., *Polym. Proc. Eng.* (1986) 4(2–4), p. 359
15. Udipi, K., *J. Appl. Polym. Sci.* (1988) 36(1), p. 117
16. Furukawa, J., Tsuruta, T., Sakata, R., Saegusa, T., *Makromol. Chem.* (1959) 32, p. 90
17. Hall, H.K., *J. Am. Chem. Soc.* (1958) 80, p. 6412
18. Tomalia, D.A., Sheetz, D.P., *J. Polym. Sci.* (1966) Part A-1, 4, p. 2253
19. Harwood, H.J., Patel, N.K., *Macromolecules* (1968) 1, p. 233
20. Sawada, H., *J. Macromol. Sci. Rev. Macromol. Chem.* (1970) C5, p. 151
21. Dainton, F.S., Ivin, K.J., *Quart. Rev.* (1958) 12, p. 82
22. Brunelle, D.J., In *Ring Opening Polymerization*. Brunelle, D.J., ed. (1995) Hanser, Munich, Chapter 11

23. Udipi, K., Davé, R.S., Kruse, R.L., Stebbins, L.R., *Polymer* (1997) 38(4), p. 927
24. Davé, R.S., Udipi, K., Kruse, R.L., Stebbins, L.R., *Polymer* (1997) 38(4), p. 939
25. Davé, R.S., Udipi, K., Kruse, R.L., Williams, D.E., *Polymer* (1997) 38(4), p. 949
26. Brzezinska, K., Szymanski, R., Kubisa, P., Penczek, S., *Makromol. Chem.-Rapid Commun.* (1986) 7, p. 1
27. Endo, M., Aida, T., Inoue, S., *Macromolecules* (1987) 20, p. 2982
28. Dreyfuss, P., Dreyfuss, M.P., *Ring Opening Polymerization*. Frisch, K.C., Reegen, S.L., eds. (1969) Marcel Dekker, New York, Chapter 2
29. Furukawa, J., Tada, K., *Ring Opening Polymerization*. Frisch, K.C., Reegen, S.L., eds. (1969) Marcel Dekker, New York, Chapter 3
30. Schulz, R.C., Hellermann, W., Nienburg, J., *Ring Opening Polymerization*. Ivin, K.J., Saegusa, T., eds. (1984) Elsevier Applied Science Publishers, New York, Chapter 6
31. Ivin, K.J., *Ring Opening Polymerization*. Ivin, K.J., Saegusa, T., eds. (1984) Elsevier Applied Science Publishers, New York, Chapter 3
32. Saotome, K., *Kogyo Kagaku Zasshi* (1962) 65, p. 402
33. Taniyama, M., Nagaoka, T., Takata, T., Sayama, K., *Kogyo Kagaku Zasshi* (1962) 65, p. 415
34. Taniyama, M., Nagaoka, T., Takata, T., Sayama, K., *Kogyo Kagaku Zasshi* (1962) 65, p. 419
35. Nagaoka, T., Takata, T., Sayama, K., Taniyama, M., *Kogyo Kagaku Zasshi* (1962) 65, p. 422
36. Shpital'nyi, A.S., Shpital'nyi, M.A., Yablochnik N.S., *J. Appl. Chem. USSR* (1959) 32(3), p. 647
37. Yoda, N., Miyake, A., *J. Polym. Sci.* (1960) 43, p. 117
38. Park, J.H., Jung, B., Choi, S.K., *Taehan Hwahakhoe-Chi* (1980) 24, p. 167 [*Chem. Abstr.* (1980) 93, p. 132897]
39. Cefelin, P., Sebenda, J., *Collect. Czech. Chem. Communs.* (1961) 26, p. 3028
40. Yumoto, H., Ogata, N., *Bull. Chem. Soc. Japan* (1958) 31, p. 913
41. Fukumoto, O., Kobayashi, R., Kunimichi, T., Japanese Patent 6213794 (1962)
42. Solomon, O., Oprescu, Cr., *Makromol. Chem.* (1969) 126, p. 197
43. Mahajan, S.S., Roda, J., Kralicek, J., *Angew. Makromol. Chem.* (1979) 75, p. 63
44. Chuchma, F., Bosticka, A., Roda, J., Kralicek, J., *Makromol. Chem.* (1979) 180, p. 1849
45. Ostaszewski, B., Wlodarczyk, M., Wlodarczyk, K., *Zesz. Nauk. Politech. Lodz., Chem.* (1976) 32, p. 136 [*Chem. Abstr.* (1977) 86, p. 90375]
46. Tani, H., Konomi, T., Japanese Patent 6929069 (1969)
47. Sekiguchi, H., Rapacoulia, P., Coutin, B., French Patent 2138228 (1973)
48. Ney, W.O., U.S. Patent 2973343 (1961)
49. Schmidt, W., German Patent 1203465 (1966)
50. Sakata, A., Mizuno, K., Isozaki, F., Japanese Patent 7226195 (1972)
51. Kobayashi, F., Sakata, A., Mizuno, K., Isozaki, F., Japanese Patent 7201222 (1972)
52. Barnes, A.C., Barnes, C.E., U.S. Patent 4217442 (1980)
53. Fiala, F., Kralicek, J., *Angew. Makromol. Chem.* (1977) 63, p. 105
54. Puffr, R., Sebenda, J., *Europ. Polym. J.* (1972) 8, p. 1037
55. Sebenda, J., *Lactam-Based Polyamides*. Puffr, R., Kubanek, V., eds. (1991) 1, Chapter 2, CRC Press, Boca Raton, Florida, p. 29
56. Sekiguchi, H., *Ring-Opening Polymerization*. Ivin, K.J., Saegusa, T., eds. 2, (1984) Elsevier, London, p. 809
57. Greenley, R.Z., Stauffer, J.C., Kurz, J.E., *Macromolecules* (1969) 2, p. 561
58. Sittler, E., Sebenda, J., *Coll. Czech. Chem. Comm.* (1968) 33, p. 270
59. Rigo, A., Fabbri, G., Talamini, G., *J. Polym. Sci. Polym. Lett. Ed.* (1975) 13, p. 469
60. Malkin, A.V., Frolov, V.G., Ivanova, A.N., Andrianova, Z.S., *Polym. Sci. USSR* (1979) 21, p. 691
61. Bolgov, S.A., Begishev, V.P., Malkin, A.Y., Frolov, V. G., *Polym. Sci. USSR* (1981) 23, p. 1485
62. Malkin, A.V., Ivanova, S.L., Frolov, V.G., Ivanova, A.N., Andrianova, Z.S., *Polymer* (1982) 23, p. 1791
63. Wittmer, P., Gerrens, H., *Makromol. Chem.* (1965) 89, p. 27
64. Sibal, P.W., Camargo, R.E., Macosko, C.W., *Polym. Process Eng.* (1984) 1, p. 147